


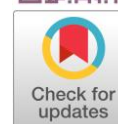


## Composite catalysts based on the CaO–Fe<sub>2</sub>O<sub>3</sub> system for the oxidative conversion of methane

Nadezhda Kirik\* , Evgenii Rabchevskii, Nina Shishkina,  
Leonid Solovyov , Alexander Anshits 

Institute of Chemistry and Chemical Technology SB RAS, Federal Research Center "Krasnoyarsk Science Center SB RAS", Krasnoyarsk 660036, Russia

\* Corresponding author: [kiriknp@icct.ru](mailto:kiriknp@icct.ru)



This paper belongs to a Regular Issue.

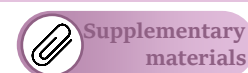
### Abstract

The catalysts of the CaO–Fe<sub>2</sub>O<sub>3</sub> system with Fe<sub>2</sub>O<sub>3</sub> content in the range of 0–100 wt.% were synthesized by the solid state method at 900 and 1000 °C. The catalysts were characterized by XRD and SEM–EDX methods, and their activity in the oxidative conversion of methane at 750 °C was studied. The phase composition of the catalysts corresponds to the CaO–Ca<sub>2</sub>Fe<sub>2</sub>O<sub>5</sub>, Ca<sub>2</sub>Fe<sub>2</sub>O<sub>5</sub>–CaFe<sub>2</sub>O<sub>4</sub> and CaFe<sub>2</sub>O<sub>4</sub>–α-Fe<sub>2</sub>O<sub>3</sub> regions of the phase diagram. The specific catalytic activity dependence on the Fe<sub>2</sub>O<sub>3</sub> content has an extremum. The CaO–Ca<sub>2</sub>Fe<sub>2</sub>O<sub>5</sub> catalysts have the highest reactivity and the active centers in them are localized at the phase interface. The activity of Ca<sub>2</sub>Fe<sub>2</sub>O<sub>5</sub>–CaFe<sub>2</sub>O<sub>4</sub> samples decreases with an increase in the CaFe<sub>2</sub>O<sub>4</sub> content. The CaFe<sub>2</sub>O<sub>4</sub>–α-Fe<sub>2</sub>O<sub>3</sub> catalysts have a core-shell structure and exhibit the least activity, which is determined by the CaFe<sub>2</sub>O<sub>4</sub> shell.

### Key findings

- Of the studied compositions in the CaO–Fe<sub>2</sub>O<sub>3</sub> system, the catalysts CaO–Ca<sub>2</sub>Fe<sub>2</sub>O<sub>5</sub> have the greatest activity in the methane oxidative conversion.

© 2024, the Authors. This article is published in open access under the terms and conditions of the Creative Commons Attribution (CC BY) license (<http://creativecommons.org/licenses/by/4.0/>).



## 1. Introduction

Oxide systems based on the calcium ferrites due to such physicochemical properties as high-temperature stability, ability to transport oxygen ions, and mixed ion-electron conductivity are widely studied as catalysts for the hydrocarbons and CO oxidation [1, 2] and as oxygen carriers for high-temperature cyclic processes, including fuels combustion [3], gasification of coal [4–6] and biomass [7, 8], hydrogen generation [9, 10], etc. An important advantage of calcium ferrite based catalysts over other oxidation catalysts is their high activity at low cost. However, systematic studies of the relationship between the composition, structural characteristics and activity of calcium ferrite catalysts have not been carried out. In this paper, the influence of the composition of the CaO–Fe<sub>2</sub>O<sub>3</sub> catalysts with varying Fe<sub>2</sub>O<sub>3</sub> content in the range of 0–100 wt.% on the activity in the oxidative methane conversion was studied.

## 2. Experimental

The catalysts of the CaO–Fe<sub>2</sub>O<sub>3</sub> system were synthesized using Fe<sub>2</sub>O<sub>3</sub> of the "high purity" qualification (TU 6-09-1418-78) and CaO of the "pure" qualification (GOST 8677-66). The reagents were mixed and ground in the required proportion using a KM-1 ball mill for an hour; the ground sample was pressed (pressure of 3.5·10<sup>3</sup> kg/cm<sup>2</sup>, exposure time of 1.5–3 min) into tablets with a diameter of 17 mm and a thickness of 1–2 mm. The tablets were calcined at 900 °C for 10 h or at 1000 °C for 4 h, and then cooled to room temperature at a rate of ~8 °C/min. The resulting tablets were crushed to obtain a fraction of 0.1–0.2 mm. The samples were denoted as xx% Fe<sub>2</sub>O<sub>3</sub>, where xx is the mass content of Fe<sub>2</sub>O<sub>3</sub> in the initial charge, for example, a sample of 57% Fe<sub>2</sub>O<sub>3</sub> contains 57 wt.% Fe<sub>2</sub>O<sub>3</sub>, and a sample of 100% Fe<sub>2</sub>O<sub>3</sub> corresponds to pure hematite treated according to the described procedure.

### Keywords

catalysts  
calcium ferrites  
solid state synthesis  
oxidative methane conversion

Received: 04.07.24

Revised: 07.08.24

Accepted: 12.08.24

Available online: 29.08.24

The quantitative phase composition of the samples and the microstructural characteristics of the phases were determined using an X'Pert PRO MPD diffractometer (PANalytical, Netherlands) with a PIXcel solid-state detector (Co K $\alpha$ ) at room temperature and 750 °C. The results were processed using a full-profile analysis of polycrystalline substances using the Rietveld method and the method of minimizing the derivative difference [11].

The specific surface area of the samples was determined using the NOVA 3200e sorption analyzer (Quantachrome Instruments, USA) in the low-temperature nitrogen adsorption mode at -195.8 °C. The calculation of the specific surface area ( $S_{sp.}$ ) was performed using the modified BET method in accordance with the international standard [12].

The surface composition and morphology of the catalyst particles were studied using a TM-3000 and TM-4000 scanning electron microscopes (Hitachi, Japan) with an energy dispersive X-ray spectrometer (EDX) Bruker XFlash 430H (Germany) equipped with a Quantax 70 microanalysis system. The accumulation time, which was at least 10 min, was determined by the quality of the spectrum assembly, which allows quantitative processing. The polished tablets or fractions of 0.1–0.2 mm of the samples were examined.

The catalytic activity in the oxidative methane conversion was studied using the continuous-flow fixed-bed unit with a stationary catalyst layer in a quartz microreactor, with of a mixture of CH<sub>4</sub>:O<sub>2</sub>:He = 82:9:9vol.%, at a temperature of 750±0.5 °C. The analysis of the initial gas mixture and reaction products was carried out using an Agilent 7890A GC chromatograph (Agilent Technologies Inc., USA) with the following columns: "Molecular Sieve 5A", "HP Plot Al<sub>2</sub>O<sub>3</sub>", "DB-1" and "Haysep Q". The specific rates of CO<sub>2</sub>, CO and C<sub>2</sub>-hydrocarbons formation were determined at the degree of oxygen conversion  $X_{O_2} = 5$ –10%.

### 3. Results and Discussion

According to phase diagram of the CaO–Fe<sub>2</sub>O<sub>3</sub> system, the ranges 0–58.7, 58.7–74 and 74–100 wt.% of Fe<sub>2</sub>O<sub>3</sub> up to 1155 °C correspond to the regions of the phase compositions CaO–Ca<sub>2</sub>Fe<sub>2</sub>O<sub>5</sub>, Ca<sub>2</sub>Fe<sub>2</sub>O<sub>5</sub>–CaFe<sub>2</sub>O<sub>4</sub> and CaFe<sub>2</sub>O<sub>4</sub>– $\alpha$ -Fe<sub>2</sub>O<sub>3</sub>. There are stable calcium ferrites of stoichiometric composition – dicalcium ferrite, Ca<sub>2</sub>Fe<sub>2</sub>O<sub>5</sub>, containing 58.7 wt.% Fe<sub>2</sub>O<sub>3</sub>, and monocalcium ferrite, CaFe<sub>2</sub>O<sub>4</sub> containing 74 wt.% Fe<sub>2</sub>O<sub>3</sub>.

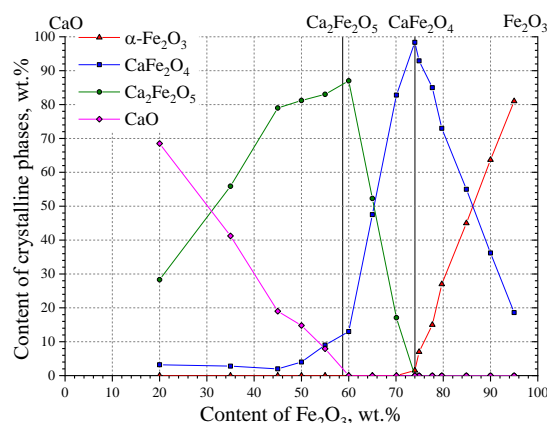
The results of the XRD phase analysis of the catalysts ( $T_{synt.} = 900$  and 1000 °C) showed a good correspondence of the Ca<sub>2</sub>Fe<sub>2</sub>O<sub>5</sub>–CaFe<sub>2</sub>O<sub>4</sub> and CaFe<sub>2</sub>O<sub>4</sub>– $\alpha$ -Fe<sub>2</sub>O<sub>3</sub> samples to the phase diagram and a slight difference in the compositions of CaO–Ca<sub>2</sub>Fe<sub>2</sub>O<sub>5</sub> catalysts from those seen in the phase diagram. The presence of CaFe<sub>2</sub>O<sub>4</sub> phase in the CaO–Ca<sub>2</sub>Fe<sub>2</sub>O<sub>5</sub> samples,  $T_{synt.} = 900$  °C, (Figure 1) is due to kinetic limitations, since the Ca<sub>2</sub>Fe<sub>2</sub>O<sub>5</sub> ferrite formation proceeds through the formation of CaFe<sub>2</sub>O<sub>4</sub> ferrite [13].

This is confirmed by the fact that among the samples in synthesized at 1000 °C, CaFe<sub>2</sub>O<sub>4</sub> ferrite was detected only when the Fe<sub>2</sub>O<sub>3</sub> content was greater than 45 wt.%. The XRD patterns of 90, 65 and 45% Fe<sub>2</sub>O<sub>3</sub> samples ( $T_{synt.} = 1000$  °C) are shown in Figures S1–S3.

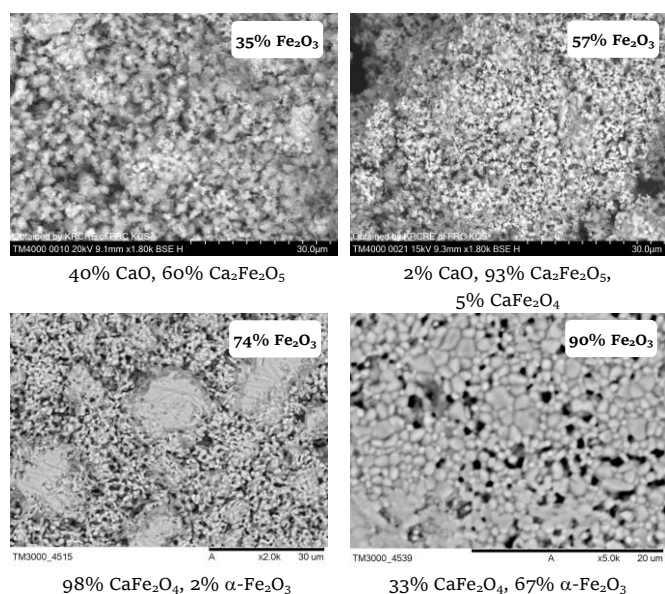
The specific surface area ( $S_{sp.}$ ) values of the samples synthesized at 900 °C vary between 0.8 and 1.5 m<sup>2</sup>/g. At  $T_{synt.} = 1000$  °C samples have a slightly smaller  $S_{sp.}$  (0.2–1.0 m<sup>2</sup>/g), while the surface of the samples with the composition CaO–Ca<sub>2</sub>Fe<sub>2</sub>O<sub>5</sub> varies little, within the ranges of 1.1–1.5 (900 °C) and 0.8–1.0 (1000 °C) m<sup>2</sup>/g, respectively.

In accordance with the SEM images, the morphology of the synthesized catalysts differs. Figure 2 shows the change in sample images with an increase in the content of Fe<sub>2</sub>O<sub>3</sub> in CaO–Fe<sub>2</sub>O<sub>3</sub>. Taking into account the phase composition of samples and the results of EDX analysis, the following conclusions were drawn. Practically single-phase samples 57% Fe<sub>2</sub>O<sub>3</sub> (93% Ca<sub>2</sub>Fe<sub>2</sub>O<sub>5</sub>) and 74% Fe<sub>2</sub>O<sub>3</sub> (98% CaFe<sub>2</sub>O<sub>4</sub>) have different morphological structures (Figure 2). The 57% Fe<sub>2</sub>O<sub>3</sub> sample has an almost homogeneous structure, consists of sintered particles of 0.5–3  $\mu$ m size. The 74% Fe<sub>2</sub>O<sub>3</sub> sample contains sufficiently large particles, up to 40  $\mu$ m, which consist of sintered small particles, 0.5–1  $\mu$ m, while large particles are surrounded by a "grid" of small particles. The Ca/Fe ratio determined in the local surface areas ( $d \approx 3$ –6  $\mu$ m) of both samples is close to that in the ferrite phases, with a slight excess in Ca content in the 57% Fe<sub>2</sub>O<sub>3</sub> sample.

The two-phase 35% Fe<sub>2</sub>O<sub>3</sub> sample is represented by partially sintered particles of non-spherical, more elongated shape; these particles have size from 0.5 to 2–3  $\mu$ m. There is phase contrast in the images of this sample; according to EDX results the value of the Ca/Fe ratio in the bright areas is close to that for dicalcium ferrite with a slight excess in Ca content, and in the other areas it varies from 5 to 6. Another two-phase sample, 90% Fe<sub>2</sub>O<sub>3</sub>, consists of agglomerates of densely sintered particles of 1–3  $\mu$ m in size, surrounded by less sintered particles of similar sizes. The value of the Ca/Fe ratio in agglomerates is varied in the range of 0.01–0.1, and it is between 0.4 and 0.5 in the other parts of the sample.



**Figure 1** The catalysts phase composition versus the Fe<sub>2</sub>O<sub>3</sub> content in the CaO–Fe<sub>2</sub>O<sub>3</sub> system ( $T_{synt.} = 900$  °C).



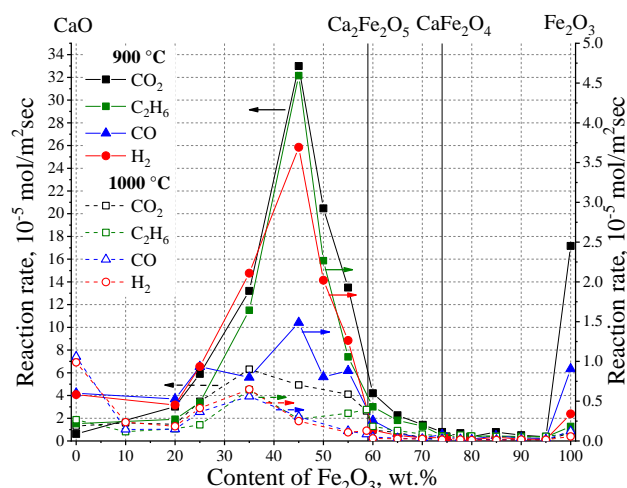
**Figure 2** The SEM images of the CaO–Fe<sub>2</sub>O<sub>3</sub> catalysts with different Fe<sub>2</sub>O<sub>3</sub> content ( $T_{\text{synt.}} = 1000\text{ °C}$ ): the catalyst particles (0.1–0.2 mm), flat surface of the 35 and 57% Fe<sub>2</sub>O<sub>3</sub> samples, and the polished tablet surface of the 74 and 90% Fe<sub>2</sub>O<sub>3</sub> samples.

One can see the EDS maps of these catalysts in Figure S4. The SEM–EDX study of catalysts synthesized at a lower temperature (900 °C) showed similar results for the samples of all compositions. It should be noted that the chemical composition, which was determined in the local surface areas of two-phase samples, does not correspond to the composition of the pure phases. In particular, it was shown that the formation of a core–shell structure is characteristic of the samples synthesized at 1000 °C with CaFe<sub>2</sub>O<sub>4</sub>– $\alpha$ -Fe<sub>2</sub>O<sub>3</sub> compositions [14].

The effect of catalysts phase composition on the activity in the oxidative conversion of methane was investigated. CO<sub>2</sub>, CO, C<sub>2</sub>H<sub>6</sub> and H<sub>2</sub> are formed at the process conditions. It can be seen (Figure 3) that the rate of product formation in the presence of the catalysts synthesized at either 900 or 1000 °C varies with the Fe<sub>2</sub>O<sub>3</sub> content.

In the region of two-phase CaO–Ca<sub>2</sub>Fe<sub>2</sub>O<sub>5</sub> samples ( $T_{\text{synt.}} = 900\text{ °C}$ ), there is no additive change in activity and phase composition. The catalytic activity curve passes through a wide maximum in the range of 25–57 wt.% Fe<sub>2</sub>O<sub>3</sub>, and the composite catalysts CaO–Ca<sub>2</sub>Fe<sub>2</sub>O<sub>5</sub> with 35–55 wt.% Fe<sub>2</sub>O<sub>3</sub> are the most active among all the catalysts. The patterns of changes in the specific activity of the active CaO–Ca<sub>2</sub>Fe<sub>2</sub>O<sub>5</sub> catalysts allow us to suppose that the active centers are localized at the interface of the phases CaO and Ca<sub>2</sub>Fe<sub>2</sub>O<sub>5</sub>. It should be noted that stoichiometric ferrite phase Ca<sub>2</sub>Fe<sub>2</sub>O<sub>5</sub> undergoes a phase transition at temperatures  $\sim 700\text{ °C}$ , in which the symmetry of the unit cell changes from primitive to body-centered [15]. The XRD study at 750 °C of the two-phase samples CaO–Ca<sub>2</sub>Fe<sub>2</sub>O<sub>5</sub> showed that phase Ca<sub>2</sub>Fe<sub>2</sub>O<sub>5</sub> in the active catalysts is also in high-temperature modification at the catalytic temperature.

The activity of the Ca<sub>2</sub>Fe<sub>2</sub>O<sub>5</sub>–CaFe<sub>2</sub>O<sub>4</sub> catalysts decreases monotonically with an increase in the content of Fe<sub>2</sub>O<sub>3</sub>, and, accordingly, with a decrease in the Ca<sub>2</sub>Fe<sub>2</sub>O<sub>5</sub> content in the sample (Figure 1).



**Figure 3** The dependences of the specific rate of product formation on the Fe<sub>2</sub>O<sub>3</sub> content in the CaO–Fe<sub>2</sub>O<sub>3</sub> system: filled point –  $T_{\text{synt.}} = 900\text{ °C}$ , empty characters –  $T_{\text{synt.}} = 1000\text{ °C}$ .

The two-phase catalysts of the CaFe<sub>2</sub>O<sub>4</sub>– $\alpha$ -Fe<sub>2</sub>O<sub>3</sub> compositions have the least activity, while the formation rates of all products differ slightly and vary within small limits. The CO<sub>2</sub> and CO formation rates increase (as well as the formation rates of H<sub>2</sub> and C<sub>2</sub>H<sub>6</sub> increase slightly) in the presence of single-phase hematite  $\alpha$ -Fe<sub>2</sub>O<sub>3</sub> sample, which belongs to the catalysts of deep oxidation of methane [16]. It is noteworthy that the activity of the CaFe<sub>2</sub>O<sub>4</sub>– $\alpha$ -Fe<sub>2</sub>O<sub>3</sub> catalysts (74–95 wt.% Fe<sub>2</sub>O<sub>3</sub>) differs slightly regardless of the phase composition. As can be seen from the results of Figure 1, the  $\alpha$ -Fe<sub>2</sub>O<sub>3</sub> content in these catalysts varies in a wide range, from 1.5 to 81 wt.%. The appearance of the hematite phase in the catalyst composition and an increase in its content does not lead to an additive increase in the catalytic properties. Consequently, the low specific activity of CaFe<sub>2</sub>O<sub>4</sub>– $\alpha$ -Fe<sub>2</sub>O<sub>3</sub> catalysts in the entire range of compositions is determined by the CaFe<sub>2</sub>O<sub>4</sub> phase, which confirms the assumption of the core–shell structure formation in these catalysts, where the CaFe<sub>2</sub>O<sub>4</sub> phase is a shell, based on the SEM–EDX results.

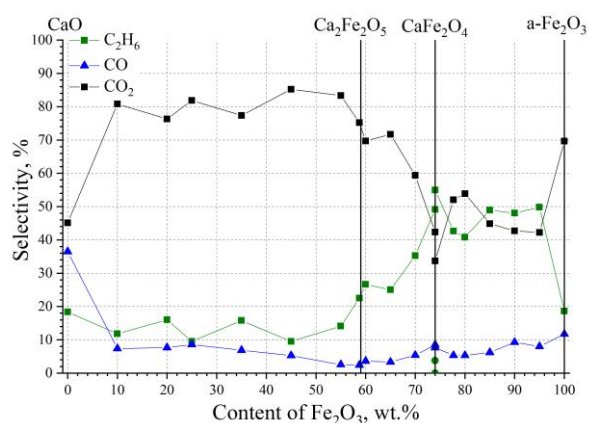
An increase in the synthesis temperature of catalysts to 1000 °C does not change the nature of the activity dependence (Figure 3), but leads to its decrease; at the points of maximum activity it is lower by more than 5 times. The high activity of low-temperature samples is apparently due to the formation of a more disordered Ca<sub>2</sub>Fe<sub>2</sub>O<sub>5</sub> phase with more mobile lattice oxygen, as evidenced by the large values of the  $b$  parameter of the unit cell of Ca<sub>2</sub>Fe<sub>2</sub>O<sub>5</sub> calculated from the XRD data. The  $b$  parameter varies in the ranges of 14.7830–14.7907 and 14.7759–14.7848 Å for the samples synthesized at 900 and 1000 °C, respectively. Ferrite Ca<sub>2</sub>Fe<sub>2</sub>O<sub>5</sub> has an orthorhombic structure of the brownmillerite-type, in which the octahedral layers alternate with the tetrahedral ones along the crystallographic axis  $b$  [15]. An increase in the values of parameter  $b$  indicates an elongation of Fe–O bonds, which leads to greater mobility of the apical oxygen (O<sub>ap</sub>) atoms in octahedra's [17].

The selectivity of product formation (S) during the methane conversion on catalysts of the CaO–Fe<sub>2</sub>O<sub>3</sub> oxide system is also different, which is well observed for the catalysts synthesized at 1000 °C (Figure 4). The most active catalysts of the CaO–Ca<sub>2</sub>Fe<sub>2</sub>O<sub>5</sub> compositions have high selectivity to CO<sub>2</sub> (S<sub>CO2</sub>), 77–85%; S<sub>CO</sub> and S<sub>C<sub>2</sub>H<sub>6</sub></sub> varies in the ranges of 3–8 and 10–16, respectively. An increase in the CaFe<sub>2</sub>O<sub>4</sub> content in Ca<sub>2</sub>Fe<sub>2</sub>O<sub>5</sub>–CaFe<sub>2</sub>O<sub>4</sub> catalysts leads to a decrease in S<sub>CO2</sub> and an increase in S<sub>C<sub>2</sub>H<sub>6</sub></sub>; values tend to selectivities of CaFe<sub>2</sub>O<sub>4</sub>–α-Fe<sub>2</sub>O<sub>3</sub> catalysts, in the presence of which S<sub>CO2</sub> and S<sub>C<sub>2</sub>H<sub>6</sub></sub> vary in ranges 43–54% and 40–58%. The catalysts synthesized at 900 °C have significantly different activity (Figure 3), while there is little difference in the selectivity of product formation (Figure S5). The S<sub>CO2</sub> varies in the range of 71–82% for the catalysts with a content of 20–95% Fe<sub>2</sub>O<sub>3</sub>. The reason for the high selectivity to CO<sub>2</sub> of the CaFe<sub>2</sub>O<sub>4</sub>–α-Fe<sub>2</sub>O<sub>3</sub> catalysts may be an increase in the contribution of the heterogeneous oxidation stage of both the CH<sub>3</sub>-radical formed on the catalyst surface during activation of the methane molecule and the oxidation of the ethane molecule formed from two CH<sub>3</sub>-radicals.

Thus, a study of the catalysts activity of the CaO–Fe<sub>2</sub>O<sub>3</sub> oxide system ( $T_{\text{synt.}} = 900$  and  $1000$  °C) in the oxidative conversion of methane at 750 °C showed that the most active catalysts are CaO–Ca<sub>2</sub>Fe<sub>2</sub>O<sub>5</sub> composite samples with a Fe<sub>2</sub>O<sub>3</sub> content of 35–55 wt.%, which have a S<sub>CO2</sub> of up to 85% and are more active compared with pure hematite, which is a catalyst of the deep methane oxidation.

## 4. Limitations

In high-temperature oxidation of hydrocarbons using complex oxide catalysts and molecular oxygen as an oxidizer, it is possible to proceed through the stages of selective and non-selective hydrocarbons conversion due to the participation of different active oxygen species/centers formed on the catalyst surface under reaction conditions. Establishing the real nature of the active centers is a difficult task that requires the use of experimental, including *in situ*, methods to study the surface state. We are going to study the catalysts' surface using the X-ray Photoelectron and Raman spectroscopy methods.



**Figure 4** The dependences of products selectivity on the Fe<sub>2</sub>O<sub>3</sub> content in the CaO–Fe<sub>2</sub>O<sub>3</sub> system,  $T_{\text{synt.}} = 1000$  °C.

## 5. Conclusions

The catalysts of the CaO–Fe<sub>2</sub>O<sub>3</sub> oxide system with a variation of the Fe<sub>2</sub>O<sub>3</sub> content from 0 to 100 wt.% were synthesized by the solid state method at 900 and 1000 °C. It was found that the specific activity of the catalysts in the oxidative conversion of methane at 750 °C varies and depends on the content of ferrite phases and their ratio.

The specific rate formation of C<sub>2</sub>-hydrocarbons, CO and CO<sub>2</sub> in the presence of Ca<sub>2</sub>Fe<sub>2</sub>O<sub>5</sub>–CaFe<sub>2</sub>O<sub>4</sub> and CaFe<sub>2</sub>O<sub>4</sub>–α-Fe<sub>2</sub>O<sub>3</sub> catalysts is lower compared with the catalysts based on CaO–Ca<sub>2</sub>Fe<sub>2</sub>O<sub>5</sub>. The activity of the latter samples is due to the centers stabilized at the phase interface CaO/Ca<sub>2</sub>Fe<sub>2</sub>O<sub>5</sub>. The ferrite phase Ca<sub>2</sub>Fe<sub>2</sub>O<sub>5</sub> has a high-temperature modification with a body-centered lattice at the catalysis temperature. The two-phase catalysts of the CaO–Ca<sub>2</sub>Fe<sub>2</sub>O<sub>5</sub> compositions with  $T_{\text{synt.}} = 900$  and  $1000$  °C, have a high activity in deep oxidation of CH<sub>4</sub>, while having a low, 10–16%, selectivity for C<sub>2</sub>H<sub>6</sub>.

The CaFe<sub>2</sub>O<sub>4</sub>–α-Fe<sub>2</sub>O<sub>3</sub> catalysts with a core-shell structure possess low activity in the conversion of methane; the activity is determined by the shell that consists of CaFe<sub>2</sub>O<sub>4</sub>.

The synthesis of the samples at a higher temperature (1000 °C) leads to a decrease of the specific activity of all catalyst compositions, but increases the selectivity of ethane formation to 55% of the CaFe<sub>2</sub>O<sub>4</sub>–α-Fe<sub>2</sub>O<sub>3</sub> catalysts.

The obtained results can be used in the development of catalytic systems based on calcium ferrites for high-temperature oxidation processes and chemical looping processes such as fuel combustion, coal and biomass gasification, hydrogen generation, etc.

## • Supplementary materials

This manuscript contains supplementary materials, which are available on the corresponding online page.

## • Funding

This work was conducted within the framework of the budget project FWES–2021–0013 for ICCT SB of the Russian Academy of Sciences using (for SEM–EDS study) the equipment of Krasnoyarsk Regional Research Equipment Center of SB RAS, and had no external funding.

## • Acknowledgments

The authors would like to thank Dr. Zhizhaev A.M. and Dr. Mazurova E.V. for their help in obtaining SEM images and analyzing of the results.

## • Author contributions

Conceptualization: N.K., A.A.

Data curation: A.A., N.K.

Investigation: N.Sh., E.R., L.S.

Methodology: N.K., E.R., L.S.

Software: E.R., L.S.

Supervision: N.K., A.A.

Validation: N.K., N.Sh., E.R., L.S.

Visualization: E.R., L.S.

Writing – original draft: N.K.

Writing – review & editing: N.K., A.A.

## ● Conflict of interest

The authors declare no conflict of interest.

## ● Additional information

Author IDs:

Nadezhda Kirik, Scopus ID [6602452315](#);

Evgenii Rabchevskii, Scopus ID [8202265100](#);

Nina Shishkina, Scopus ID [6701911079](#);

Leonid Solovyov, Scopus ID [6701367459](#);

Alexander Anshits, Scopus ID [57200009289](#).

Website:

Federal Research Center "Krasnoyarsk Science Center SB RAS", <https://ksc.krasn.ru/en/>.

## References

- Hirabayashi D, Yoshikawa T, Kawamoto Y, Mochizuki K, Suzuki K. Characterization and applications of calcium ferrites based materials containing active oxygen species. *Adv Sci Technol.* 2006;45:2169–2176. doi:[10.4028/www.scientific.net/AST.45.2169](#)
- Isupova LA, Tsybulya SV, Kryukova GN, Budneva AA, Paukshtis EA, Litvak GS, Ivanov VP, Kolomiichuk VN, Pavlyukhin YuT, Sadykov VA. Mechanochemical synthesis and catalytic properties of the calcium ferrite  $\text{Ca}_2\text{Fe}_2\text{O}_5$ . *Kinet Catal.* 2002;43(1):132–139. doi:[10.1023/A:1014217716883](#)
- Ismail M, Liu W, Dunstan MT, Scott SA. Development and performance of iron based oxygen carriers containing calcium ferrites for chemical looping combustion and production of hydrogen. *Int J Hydrogen Energ.* 2016;41:4073–4084. doi:[10.1016/j.ijhydene.2015.11.066](#)
- Siriwardane R, Riley J, Tian H, Richards G. Chemical looping coal gasification with calcium ferrite and barium ferrite via solid–solid reactions. *Appl Energy.* 2016;165:952–966. doi:[10.1016/j.apenergy.2015.12.085](#)
- Miller DD, Siriwardane R.  $\text{CaFe}_2\text{O}_4$  oxygen carrier characterization during the partial oxidation of coal in the chemical looping gasification application. *Appl Energy.* 2018;224:708–716. doi:[10.1016/j.apenergy.2018.05.035](#)
- Zhang J, He T, Wang Z, Zhu M, Zhang K, Li B, Wu J. The search of proper oxygen carriers for chemical looping partial oxidation of carbon. *Appl Energy.* 2017;190:1119–1125. doi:[10.1016/j.apenergy.2017.01.024](#)
- Riley J, Siriwardane R, Tian H, Benincosa W, Poston J. Kinetic analysis of the interactions between calcium ferrite and coal char for chemical looping gasification applications: Identifying reduction routes and modes of oxygen transfer. *Appl Energy.* 2017;201:94–110. doi:[10.1016/j.apenergy.2017.05.101](#)
- Huang B-S, Chen H-Y, Chuang K-H, Yang R-X, Wey M-Y. Hydrogen production by biomass gasification in a fluidized bed reactor promoted by an Fe/CaO catalyst. *Int J Hydrogen Energ.* 2012;37:6511–6518. doi:[10.1016/j.ijhydene.2012.01.071](#)
- Sun Zh, Chen Sh, Hu J, Chen A, Rony AH, Russell ChK, Xiang W, Fan M, Dyar MD, Elizabeth C, Dklute EC.  $\text{Ca}_2\text{Fe}_2\text{O}_5$ : A promising oxygen carrier for  $\text{CO}/\text{CH}_4$  conversion and almost pure  $\text{H}_2$  production with inherent  $\text{CO}_2$  capture over a two-step chemical looping hydrogen generation process. *Appl Energy.* 2018;211:431–442. doi:[10.1016/j.apenergy.2017.11.005](#)
- Ismail M, Liu W, Chan MSC, Dunstan MT, Scott SA. Synthesis, application, and carbonation behavior of  $\text{Ca}_2\text{Fe}_2\text{O}_5$  for chemical looping  $\text{H}_2$  production. *Energy Fuels.* 2016;30(8):6220–6232. doi:[10.1021/acs.energyfuels.6b00631](#)
- Solovyov LA. Full-profile refinement by derivative difference minimization. *J Appl Cryst.* 2004;37:743–747. doi:[10.1107/S0021889804015638](#)
- ISO 9277:2010-09 (E). Determination of the specific surface area of solids by gas adsorption – BET method. 2010.
- Berezhnoi AS. *Mnogokomponentnye sistemi oksidov [Multi-component oxide systems]*. Kiev: Naukova dumka; 1970. P.97. Russian.
- Knyazev YuV., Shishkina NN., Bayukov OA., Kirik NP., Solovyov LA., Anshits AG. Cation distribution in the composite materials of the  $\text{CaFe}_2\text{O}_4$ - $\alpha$ - $\text{Fe}_2\text{O}_3$  series. *Russ J Struct Chem.* 2019;60(5):763–771. doi:[10.1134/S0022476619050081](#)
- Shaula AL, Pivak YV, Waerenborgh JC, Gaczyński P, Yaremchenko AA, Kharton VV. Ionic conductivity of brownmillerite-type calcium ferrite under oxidizing conditions. *Solid State Ionics.* 2006;177:2923–2930. doi:[10.1016/j.ssi.2006.08.030](#)
- Popovskii VV. Regular features of total oxidation over solid oxide catalysts. *Kinet. Katal.* 1972;13(5):1190–1203.
- Paulus W, Schober H, Eibl S, Johnson M, Berthier T, Hernandez O, Ceretti M, Plazanet M, Conder K, Lamberti C. Lattice dynamics to trigger low temperature oxygen mobility in solid oxide ion conductors. *J Am Chem Soc.* 2008;130:16080–16085. doi:[10.1021/ja806144a](#)